Timescales of Galaxy Mergers and Satellite Stripping

Abstract

In this work we investigate the merging times and rates of mass accretion in binary mergers between galaxies that consist of a dark matter halo and a stellar bulge. We present our own definition of the merging time and test the formula presented in [Boylan-Kolchin et al., 2008] against the results of 15 N-body simulations. In particular we examine the accuracy of the formula when the merging time is measured from when the satellite is separated from the host by a radius $r < r_{\mathrm{vir}}$. In addition we analyse the rates of dark matter and stellar accretion to the host galaxy. We find that the predictions from [Boylan-Kolchin et al., 2008] are systematically longer than our measured timescales and that the difference is due to the sensitivity of the definitions of the merging time to the mass loss of the satellite. We conclude that, in spite of the disagreement with our measurements, the formula in [Boylan-Kolchin et al., 2008] is consistent for $r < r_{\mathrm{vir}}$. From our analysis of mass accretion we have two main results. Firstly, stellar mass is accreted slowly (by $\approx 10\%$ or less) until the halo of the satellite is diminished by $\approx 90\%$, after which it is accreted quickly. Secondly, the rate of stellar accretion after the halo is stripped by $\approx 90\%$ depends on the initial mass and trajectory of the satellite. We hope that our work will be useful to semi-analytic models of structure formation and to observations of merging pairs.

Bryn Elesedy

Supervised by Ben Möster and Debora Sijacki

Contents

1 Introduction

It is a commonly held belief that the large scale structure of the Universe, including galaxies, formed hierachically from the coalescence of smaller substructures. At very early times, about $t \sim 10^{-36}$ seconds after the Big Bang, the Universe was so small that quantum effects were relevant to its gross structure and lead to perturbations in its density field. Rapid inflation then dispersed the perturbations into causally disconnected regions of spacetime. Initially the gravitationally bound perturbations grew in extent with the expansion of the universe. However, when they reached $\delta\rho/\rho \sim 1$ they began to collapse under their own self-gravity. The popular ΛCDM paradigm asserts that each of these initial perturbations contains both baryonic and dark matter, roughly in their cosmic proportions. From these over-densities, dark matter collects and collapses to form halos, while cool gas condenses and collapses violently to form stars — this is the genesis of galaxies as we know them [Mo and White, 2010a]. These early progenitor galaxies then clustered and mergered hierachically to form ever larger structures, with the remnants that we see today bearing the scars of their past (e.g. [White and Rees, 1978] and [Efstathiou and Silk, 1983]). We call this process of multiple halos or galaxies interacting to form a larger body a merger and, of particular relevance to this work, we speak of a binary merger if the event involves only two progenitors. Henceforth, all references to a merger events are to binary mergers only. We will call the larger of the progenitors the host and the smaller the satellite. If the satellite is of similar size to the host ($M_{\text{sat}}/M_{\text{host}} > 0.3$), then we call the event a major merger, otherwise we name the event a minor merger.[1]

The primary physical process by which the merging of dark matter halos and galaxies occurs is dynamical friction. Dynamical friction is a purely gravitational, collisionless interaction between a mass and a diffuse body of particles.[2] In the context of galaxy mergers it manifests itself as follows: the satellite galaxy travels through the host, attracting the constituents of the host in a direction perpendicular to its trajectory. As the satellite is moving relative to the host, this creates an asymmetric distribution of host particles along the trajectory of the satellite, forming a wake. The wake then exerts a gravitational force on the satellite, reducing its velocity and causing its orbit to decay towards the centre of the host. As the satellite's orbit decays, gravitational tidal forces cause its mass to be stripped and ultimately the satellite is subsumed by the host.

Given that galaxies constitute an abundant and fundamental component of the structure of the Universe, it is clear that knowledge of merger events between galaxies and dark matter halos is pertinent to our understanding of the cosmos. Moreover, as one would imagine, the merger history of a galaxy is critical to its properties. Mergers can trigger intense nuclear reactions and star

[1] The latter of these is more common. See, for instance, [Bertone and Conselice, 2009].

[2] In this setting a star (or a bound cluster stars) would be considered a particle.

formation via the concentration of gas and can even completely transform the morphology of the galaxy, i.e. from spiral to elliptical or the emergence of tidal tails (e.g. [Toomre and Toomre, 1972] and [Toomre, 1977]) [Mihos, 2000]. Indeed it is thought that a fair fraction of ellipticals have formed from mergers [Barnes and Hernquist, 1992]. In turn, an understanding of the timescale of a merging process and the rate of mass accretion is important to cosmological models, especially semi-analytic models of structure formation that depend on a specified merger or accretion rate. Galaxy mergers happen over a time period much greater than the career of even the most persistent astronomer, so observations must be made by piecing together the snippets of merging processes that we see into a coherent scheme. Accurate knowledge of the timescale of mergers can therefore be critical to observations. The merging time formula proposed in [Boylan-Kolchin et al., 2008] is designed to provide estimates of merging timescales. The contribution of this work is an examination of the correctness of the formula and of the rate at which mass is accreted to the host. In particular it will give some insight into the accuracy of the formula when applied part way through a merger event.

2 Previous work on merging times

Expressions for galaxy merging times have classically been based upon considerations of dynamical friction.[3] This is intuitive, as dynamical friction is the process by which the orbit of the satellite decays. To incorporate this into models of galaxy mergers, calculations use the dynamical friction time t_{df} — the time taken for the satellite to lose all of its orbital angular momentum[4] to dynamical friction, i.e. the time taken for the orbit of the satellite to decay completely. In turn, calculations of t_{df} are generally based on the Chandrasekhar dynamical friction formula [Chandrasekhar, 1943] for a point mass M moving through an infinite, homogeneous sea of particles of mass m

$$\frac{\mathrm{d}\mathbf{v}_M}{\mathrm{d}t} = -16\,\pi^2 \ln\Lambda\, G^2\, m(M+m)\,\frac{1}{v_M^3}\int_0^{v_M} f(v_M)v_M^2\,\mathrm{d}v_M\,\mathbf{v_M} \tag{2.1}$$

where $\mathbf{v}_M$ is the velocity of the point mass, $f(v_m)$ is the isotripic velocity distribution of the particles and $\ln\Lambda$ is the ever problematic Coulomb logarithm (taken to be constant) (for details, see [Binney and Tremaine, 1987]). To arrive at an expression for t_{df} from this prescription one typically makes some assumptions. For a point satellite of mass $M_S \gg m$ on a circular orbit in a spherical, singular isothermal host that has a Maxwellian velocity distribution we arrive at

$$t_{\mathrm{df}} = \frac{1.17}{\ln\Lambda}\,\frac{r_i^2 V_c}{GM_S}, \tag{2.2}$$

where G is the gravitational constant, r_i is the initial radius from the centre of the host to the satellite, V_c is the circular velocity of the host and the Coulomb logarithm is $\ln\Lambda = \ln\left(\frac{M_{\mathrm{host}}}{M_S}\right)$, with M_{host} the mass of the host [Mo and White, 2010b].

However, there are problems with this method. Firstly, we are interested in the dynamical friction experienced by an extended body rather than a point mass, to which (2.1) is not directly applicable. This issue is addressed in [White, 1976] where, to incorporate the satellite as a rigid body, a modification is made to the velocity of the satellite in terms of the impact parameter of its encounters with host particles that gives a corresponding modification of the Coulomb logarithm (see [Mo and White, 2010b]). In spite of such modifications there are still inaccuracies in the rigid body approximation. It is shown in [Fujii et al., 2006] that the internal degrees of freedom of the satellite are significant to its orbital decay via tidal stripping. In particular, stripped material that resides in the wake of the satellite exerts drag and stripped material that remains close to the satellite enhances the wake. To clarify the second effect, more material is drawn into the wake

[3] There are groups that track halos in cosmological simulations and measure merging times. They calculate the time taken for two halos of a given separation to coalesce into a larger structure. This is subtly different from what we are interested in — the time taken for orbital decay of a satellite that is at the virial radius of the host — so will not be covered here.

[4] Unless stated otherwise, orbital angular momentum of the satellite is relative to the centre of mass of the host.

than would be drawn by the bound mass of the satellite.
Attempts have been made to rescue merging time estimates based on (2.2) by fitting a similar expression to numerical simulations. For instance, [Navarro et al., 1995] performed simulations of dark matter halos of singular isothermal sphere density distribution with gaseous cores (not including star formation). To their simulations they fitted the formula

$$T_{\mathrm{df}} = \frac{1}{2}\frac{f(\eta)}{GC\ln\Lambda}\frac{V_c r_c^2}{M_{\mathrm{sat}}} \tag{2.3}$$

where η is orbital circularity, $r_c(E)$ is the radius of the circular orbit with the same orbital energy as the satellite, M_{sat} is the mass of the satellite and $C \approx 0.43$ is constant. They found that $f(\eta) = \eta^{0.78}$ is in good agreement with their data for $\eta > 0.02$. In contrast, [Jiang et al., 2008] found a weaker dependence on orbital circularity $f(\eta) = 0.94\eta^{0.60} + 0.60$ for similar N-body/hydro simulations (albeit including star formation) and arrived at the formula

$$T_{\mathrm{merge}} = \frac{0.90\eta^{0.60} + 0.60}{2C}\frac{M_{\mathrm{host}}/M_{\mathrm{sat}}}{\ln(1 + M_{\mathrm{host}}/M_{\mathrm{sat}})}\frac{\sqrt{r_{\mathrm{vir}} r_c}}{V_c}. \tag{2.4}$$

where r_{virial} is the virial radius of the host and a choice of $\Lambda = 1 + M_{\mathrm{host}}/M_{\mathrm{sat}}$. They cite imprecisions in the Coulomb logarithm as a key source of discrepancy with [Navarro et al., 1995].

In a slightly different vein, [Boylan-Kolchin et al., 2008] use the fitting formula

$$\frac{\tau_{\mathrm{merge}}}{\tau_{\mathrm{dyn}}} = A\,\frac{(M_{\mathrm{host}}/M_{\mathrm{sat}})^b}{\ln(1 + M_{\mathrm{host}}/M_{\mathrm{sat}})}\exp\left(c\,\frac{j}{j_c(E)}\right)\left(\frac{r_c(E)}{r_{\mathrm{vir}}}\right)^d \tag{2.5}$$

where $\tau_{\mathrm{dyn}} = r_{\mathrm{vir}}/V_c(r_{\mathrm{vir}})$ is the dynamical time of the satellite at the virial radius of the host and j is the specific orbital angular momentum of the satellite relative to the host's centre of mass. Note that this is a much stronger dependence on the orbital circularity $\eta = j/j_c(E)$ than above. They fit (2.5) to simulations of dry mergers (no gas) between [Hernquist, 1990] profile dark matter halos and find $A = 0.216$, $b = 1.3$, $c = 1.9$ and $d = 1.0$. Further, the formula (2.5) is tested against simulations that include stellar bulges and a $\approx 10\%$ reduction to τ_{merge} is suggested for these systems. This report will extend upon the work of [Boylan-Kolchin et al., 2008].

3 Methods

3.1 Simulations

3.1.1 The set up

We ran 15 gravitational N-body simulations to test

$$\frac{\tau_{\rm merge}}{\tau_{\rm dyn}} = 0.216\, \frac{(M_{\rm host}/M_{\rm sat})^{1.3}}{\ln(1 + M_{\rm host}/M_{\rm sat})} \exp\left(1.9\, \frac{j}{j_c(E)}\right) \frac{r_c(E)}{r_{\rm vir}} \tag{3.1}$$

against dry, binary merger systems of galaxies that include a baryonic component, for a variety of satellite to host mass ratios and initial trajectories.[5] Henceforth we employ a 10% reduction of (3.1) to account for the baryonic component, as advised in [Boylan-Kolchin et al., 2008]. Gas or star formation are not considered in this work and our simulated mergers consist solely of gravitational interactions. Relativistic effects and the Ricci scalar are negligible for the particles in our simulations, so the dynamics of the system are governed entirely by Newtonian gravity. Moreover, our analysis of mergers is purely numerical, with the relevant physical processes such as dynamical friction and tidal stripping arising organically from gravitational interactions. The simulations were performed using the GADGET-3 package: massively parallel code for N-body simulations [Springel, 2005]. GADGET works by splitting the volume of the simulation into smaller sub-volumes, with the size of the sub-volume dependent on the density at that point (smaller volume for more dense regions and vice-versa). Gravitational forces are then computed by multipole expansion between the individual particles in each sub-volume and between the sub-volumes themselves. Snapshots were taken every 0.1 Gya, or equivalently every $\approx 0.07\,\tau_{\rm dyn}$. The gravitational force softening (the separation at which we neglect the gravitational interaction between particles to prevent singularities) follows the scheme of [Dehnen, 2001] with $\epsilon = \epsilon_1\sqrt{M_{\rm particle}/10^{10}M_\odot}$ and a choice of $\epsilon_1 = 32\,{\rm kpc}$. We take $M_{\rm halo\ particle} = 10^6 M_\odot$ and $M_{\rm bulge\ particle} = 6\times10^4 M_\odot$, giving a dark matter softening length of $\epsilon_{\rm dm} = 0.32\,{\rm kpc}$ and bulge softening length of $\epsilon_{\rm bulge} = 0.078\,{\rm kpc}$. We use a flat cosmology with $\Omega_{\rm M} = 0.3$, $\Omega_\Lambda = 0.7$ and $H_0 = 0.7\,{\rm kms^{-1}kpc^{-1}}$. Virial quantities of the galaxies are defined in terms of the corresponding virial radius R_{200c}, the radius of a body that encloses an average density of $200\rho_{\rm crit}$, where $\rho_{\rm crit} = \frac{3H^2}{8\pi G} \approx 10^{-26}\,{\rm kg/m^3}$ is the mean density of a flat universe at the present.

[5] The simulations were carried out on the Darwin Supercomputer of the HPCS, Cambridge.

3.1.2 The galaxies

In this work we used four galaxies, each consisting of a large dark matter halo and a stellar bulge, with both components of [Hernquist, 1990] profile

$$\rho(r) = \frac{M}{2\pi} \frac{a}{r(r+a)^3} \tag{3.2}$$

where a is a constant scale length. The galaxies are named G100, G030, G010 and G005 and their key properties are listed in Table 1. The galaxies were constructed using the MakeNewDisk code, described in [Springel et al., 2005], and were evolved in isolation for 5 Gya to confirm the stability of their profile. Snapshots were taken at 0 Gya, 2.5 Gya and 5 Gya and histogram plots of the density of the galaxies were compared to the relevant Hernquist profiles.

Property		G100	G030	G010	G005
Halo	Particles	10^6	3×10^5	10^5	5×10^4
	$M/M_\odot$	10^{12}	3×10^{11}	10^{11}	5×10^{10}
	R_{200}/kpc	206	138	96	76
	a/kpc	40.0	26.8	18.5	14.7
Bulge	Particles	5×10^5	1.5×10^5	16667	3333
	$M/M_\odot$	3×10^{10}	9×10^9	10^9	2×10^8
	R_{200}/kpc	1	0.67	0.46	0.37
	a/kpc	1.0	0.67	0.46	0.37

Table 1: Properties of the galaxies used. **Particles** is the total number of particles used for that component of the galaxy in our simulations. M is the mass of that component, measured in solar masses $M_\odot$. R_{200} is the virial radius of the component. a is the constant scale length for the Hernquist profile of the component

.

3.1.3 Parameter set

The parameter set used is displayed in Table 2. In each run the satellite starts with its centre of mass at the virial radius of the host. Mass ratios were chosen to be $M_{\rm sat}/M_{\rm host} = 0.3,\ 0.1$ and 0.05. This reflects the range used in [Boylan-Kolchin et al., 2008] as well as the supposed domain of credibility of (3.1). Moreover, the range covers the most dynamically interesing scenarios. A priori estimates of merging timescales for galaxy pairs with a mass ratio much less than 1:20 often exceed a Hubble time, while for major mergers ($M_{\text{sat}}/M_{\text{host}} > 0.3$) they are closer to a dynamical time. Further still, analysis of cosmological simulations have shown that almost all galaxy mergers have $M_{\text{sat}}/M_{\text{host}} \in [0.01, 0.3]$ [Bertone and Conselice, 2009].

The initial trajectories of the galaxies are Keplerian ellipses specified by (e, r_{min}). In this work we used eccentricities $e \in [0, 0.95]$, a wide range of orbits, covering the vast majority of the distribution seen in dark matter simulations [Zentner et al., 2005], [Benson, 2005]. Once e is specified, we chose r_{min} to keep the initial value of $r_c(E)/r_{\text{vir}}$ (a parametrisation of the orbital energy) in a sensible range, where $r_c(E)$ is defined to be the radius of a circular orbit with the same energy as the satellite. In this case, a sensible range for $r_c(E)/r_{\text{vir}}$ is the restriction that it not be much greater than unity. If it is, the satellite may retain enough orbital angular momentum after its first pericentric passage to then travel many times the host's virial radius before its second pericentric passage. This would cause infeasibly long simulation times. The calculation of $r_c(E)$ was carried out using the Hernquist potential rather than the two body approximation. The mass (and therefore the potential) of the host's bulge was neglected in the calculation since $M_{\text{bulge}}/M_{\text{halo}} = 0.03 \ll 1$ and the resulting expression is

$$r_c(k) = -\frac{k}{2} - a + \frac{1}{2}\sqrt{k(k - 4a)} \tag{3.3}$$

with $k = \frac{GM}{2E}$ and a the scale length of the host's halo.

Run	$M_{\text{sat}}/M_{\text{host}}$	e	r_{min} (kpc)	Run	$M_{\text{sat}}/M_{\text{host}}$	e	r_{min} (kpc)
30:95	0.3	0.95	20	10:80	0.1	0.80	40
30:85	0.3	0.85	20	10:75	0.1	0.75	50
30:60	0.3	0.60	55	10:70	0.1	0.70	55
30:40	0.3	0.40	89	10:65	0.1	0.65	50
30:0	0.3	0	206	05:95	0.05	0.95	20
10:95	0.1	0.95	20	05:85	0.05	0.85	20
10:90	0.1	0.90	15	05:75	0.05	0.75	30
10:85	0.1	0.85	20				

Table 2: Parameter set for simulations. The initial trajectory of the satellite is a Keplerian ellipse, specified by orbital eccentricity e and pericentric distance r_{min}.

3.2 Analysis

3.2.1 Defining a merger

We define the satellite galaxy to have merged with the host when its angular momentum relative to the host's COM diminishes to below 1% of its initial value and does not surpass this value again. More specifically, we consider the merger event to have happened at time t_0 if, $\forall\, t > t_0$,

$$J(t) \equiv \mu\,[(\mathbf{r}_{\rm sat} - \mathbf{r}_{\rm host}) \times (\mathbf{v}_{\rm sat} - \mathbf{v}_{\rm host})] < \frac{1}{100}\,J(0) \tag{3.4}$$

where the positions and velocitites are of the respective centres of mass and $\mu = \frac{M_{\rm sat}M_{\rm host}}{M_{\rm sat}+M_{\rm host}}$. Note that it is possible that the satellite's angular momentum drops below this threshold, but then exceeds it again at some later time. In such cases it can be difficult to distinguish between numerical noise and the satellite genuinely retaining its identity. With this in mind, we define the error in a merging timescale measurement to be the difference between the current measurement and the time when $J(t)$ last dropped below $\frac{1}{100}J(0)$, provided that the satellite has had $J(t) \geq \frac{1}{100}J(0)$ in the interim, otherwise the error will be 0.1 Gya.

Our defintion is a departure from [Boylan-Kolchin et al., 2008], where a merging event happens when the satellite loses all of its specific angular momentum $j = rv_t$ relative to the host. According to the definition in [Boylan-Kolchin et al., 2008], the satellite will have merged with the host either when its orbit has decayed totally or when its mass has been stripped and has assumed an average velocity profile that is the same as the host's. Therefore it is possible for a satellite to have merged by our definition but not by the standard of [Boylan-Kolchin et al., 2008]: for instance it could have lost over 99% of its mass but only some of its specific angular momentum. According to the definition in [Boylan-Kolchin et al., 2008] it is possible to have only a very small section of the satellite remaining and orbiting well within the virial radius of the host, but for the merger to have not taken place. Physical intuition tells us that the galaxies have merged in these cases because the remnant of the satellite is tightly bound, close to the centre of the host and the satellite has lost much of its identity. Our definition reflects this by neglecting these very small remnants. This notion is supported by the plots in section 4.2, which show that our merging times are closely correlated with the total accretion of the satellite mass to the host.

3.2.2 Performing the analysis

In order to identify the satellite during the simulation, we used the package Subfind that is described in [Springel et al., 2001]. Subfind reads the gadget output, "identifies locally over-dense, self-bound particle groups" and records their positions, velocities and masses in another set of files for each timestep. Subfind works by first applying a friends of friends (FOF) algorithm

[Davis et al., 1985] to the simulation volume. The FOF algorithm groups the particles by their separation based on a specified linking length b as follows: Take two particles P and Q each in a group (of one or more particles), if the separation between them is less than b then the groups containing P and Q are combined. This process is carried out iteratively until all the particles closer than b are grouped accordingly (but there are no groups). The simulation volume is now subdivided regions of extent that depends on their density. SUBFIND then defines a density field for the simulation by interpolating the densities between the positions of each particle. Regions of the simulations that are locally over-dense with respect to the interpolated density field are considered as candidate halos. The particles in the candidate halos are checked for boundedness and the unbound particles are discarded. Finally, the energies of the remaining particles in the candidate halo are examined and those that are mutually self-bound and larger than a predetermined minimum resolution are catalogued as a sub-halos. For our simulations we specified the FOF linking length as 0.16 kpc and the minimum resolution as 32 particles, meaning that the minimum mass of a substructure in our simulation is set at $1.92 \times 10^6\, M_\odot$. We then collated the information from the SUBFIND output and calculated the properties of the galaxies, such as relative angular momentum and $r_c(E)$, for each timestep of the simulation. The short piece of C code that records the merging timescale and measurement error for each simulation is provided in the appendix.

All plots in this work were made using the `epslatex` terminal for `gnuplot`, a command-line driven plotting utility.

4 Results

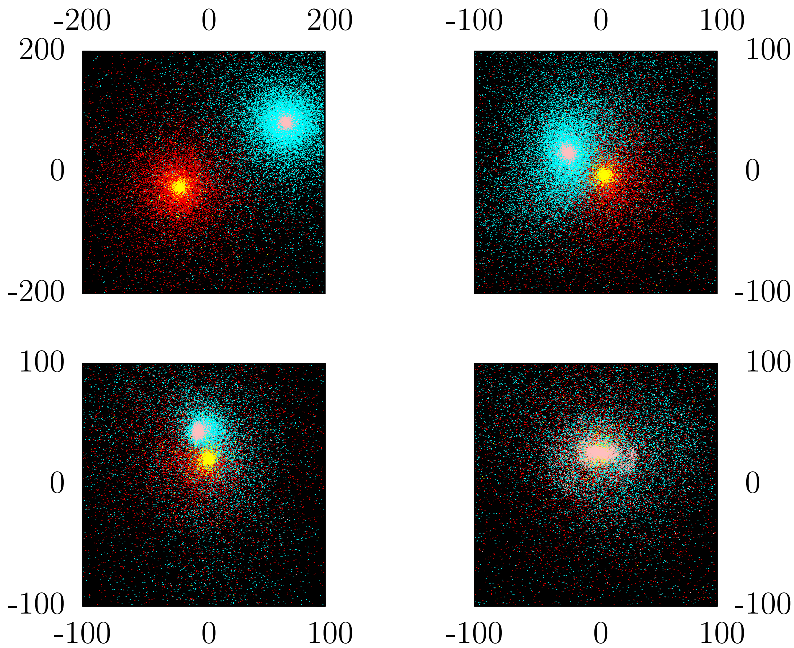

Figure 1: Run 30:85. **Lengths are in kpc**. Plots are of projections of the simulation onto the plane of motion. Halo particles are plotted in red for the host and cyan for the satellite. Bulge particles are plotted in yellow for the host and pink for the sattelite. Satellite particles are plotted five times more frequently than for the host. **Top left** shows the intial condition of the simulation, with the satellite's centre of mass at the virial radius of the host. **Top right** is the first pericentric passage at 0.7 Gya; notice the distortion in the halo of the sattelite. **Bottom left** is the second pericentric passage at 3.6 Gya, the satellite halo is almost completely stripped but the bulge remains intact. **Bottom right** is at 5 Gya. By now the system has merged and the satellite has been completely destroyed.

4.1 Merging Times

4.1.1 From the virial radius

Table 3 shows the predicted and recorded merging times for each simulation along with the initial value of the parameter $r_c(E)/r_{\rm vir}$, calculated from the SUBFIND output. The initial values for $r_c(E)/r_{\rm vir}$ are often unexpected, particularly for 30:95 (which is why the estimate of $\tau_{\rm merge}$ is so grossly incorrect). The values for runs 10:95 and 05:95 are missing altogether because SUBFIND calculated $0 < \frac{GM_{\rm host}}{2E} < 4a$ in these cases. That is, the velocity of the satellite was seen to be so great that it was unbound from the host, so there is no circular orbit of that energy.[6] The problem

[6] As an aside, had we used the two body approximation here with a $\sim 1/r$ force law, then we may not have encounter such issues because the singularity at $r = 0$ can always bind the satellite provided it passes close enough to the origin.

is that SUBFIND reads the velocity of the satellite as being much too large at the beginning of the simulation, affecting all of the runs but most severely for the trajectories of high eccentricity. The measurements become more stable and closer to what we would expect as the simulation progresses.[7]

The predicted values for τ_{merge} are significantly larger than the measured values. Even when we allow for a 10% shortening of the prediction for the inclusion of the baryonic component (see [Boylan-Kolchin et al., 2008]), with a RMS error of 5.3 Gya the predictions are contrary to our measurements. Though in spite of the numerical differences, they agree in two main aspects. Firstly, if one measurement is larger/smaller than another then the corresponding predictions are almost always larger/smaller respectively. Secondly, merging times broadly increase with increases in circularity and are inversely related to the mass ratio.

Figure 2 and Figure 3 show plots of the angular momentum of the satellites and the centre of mass separation of the galaxies in runs with $M_{\text{sat}}/M_{\text{host}} = 0.3$, while Figure 4 and Figure 5 show the same for runs 10:90, 10:80, 10:75 and 10:70. Note that pericentric passages generally coincide with sharp losses in angular momentum, especially for the smaller satellite and higher eccentricities. Conversely, the larger satellite and lower eccentricity runs exhibit a more constant loss in angular momentum. In addition, the smaller satellites have remnants that orbit the centre of mass of the host long after their halo has diminished (see Figure 10). Observe from Figure 3 that the satellite orbits do not vary markedly in circularity over time. This is concurrent with the idea that dynamical friction has no net effect on the circularity of a satellite's orbit.

In each of the plots, the plotted lines cease at different times. A line stops when SUBFIND cannot identify two distinct self-bound bodies, either because the satellite's extent has passes below the minimum resolution of SUBFIND (32 particles) or because the simulation has ended.

[7]This points a finger at SUBFIND rather than GADGET, but this is aided by the fact that the velocities of the satellites reduce anyway due to dynamical friction. It is likely that the problem lies in the way that SUBFIND uses halo data from previous snapshots as initial estimates for iterative calculations, so inaccuracies are more likely towards the beginning of the simulation, but a detailed discussion of SUBFIND is outside of the scope of this project.

Run	$(r_c(E_0)/r_{\rm vir})$	$\tau_{\rm merge}$	$(\tau_{\rm merge})_{\text{B-K}}$	Abs. Error	% Error
30:95	52	4.2 ± 0.1	55	51	1200%
30:85	0.82	2.7 ± 0.1	2.9	0.2	7.4%
30:60	0.86	4.7 ± 0.1	6.0	1.3	28%
30:40	0.97	6.5 ± 0.1	8.6	2.1	32%
30:0	1.2	8.4 ± 0.1	10	1.6	19%
10:95	—	12 ± 0.1	—	—	—
10:90	0.99	2.5 ± 0.1	6.7	4.2	170%
10:85	0.90	6.2 ± 0.1	7.3	1.1	18%
10:80	1.6	4.6 ± 0.1	14	9.4	200%
10:75	1.6	5.3 ± 0.1	15	9.7	180%
10:70	1.4	5.3 ± 0.1	15	9.7	180%
10:65	1.0	12.3 ± 0.1	14	1.7	14%
05:95	—	29.8 ± 0.1	—	—	—
05:85	0.92	10.4 ± 1.0	14	3.6	35%
05:75	0.74	13.7 ± 1.2	18	4.3	31%

Table 3: Output of simulations. $\tau_{\rm merge}$ is the measured merging time in Gya. $(\tau_{\rm merge})_{\text{B-K}}$ is the merging time predicted by (3.1) in Gya, reduced by 10% to account for baryons. Abs. Error is the absolute error in the prediction against our measurements, in Gya, and % Error is this error as a percentage of the measured merging time.

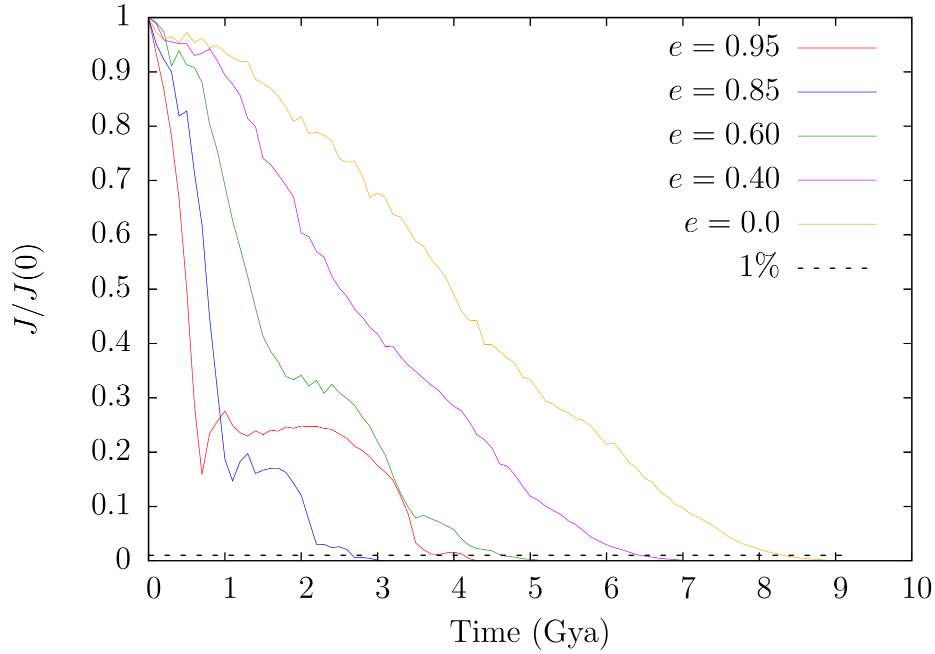

Figure 2: $M_{\mathrm{sat}}/M_{\mathrm{host}} = 0.3$: Angular momentum against time, normalized such that the $t = 0$ values are unity.

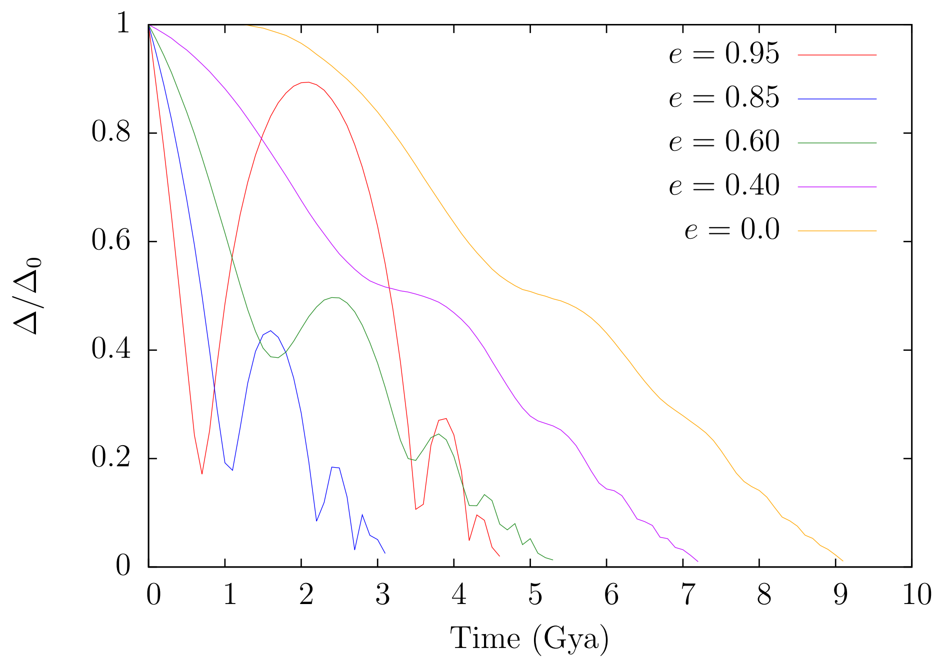

Figure 3: $M_{\mathrm{sat}}/M_{\mathrm{host}} = 0.3$: centre of mass separation between the galaxies Δ against time, normalized such that the $t = 0$ values are unity.

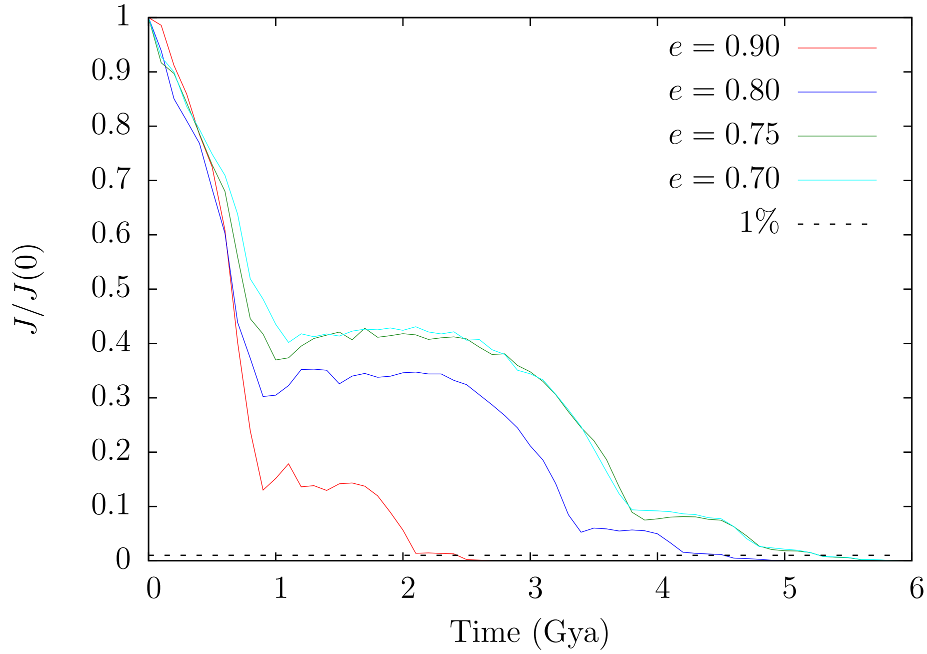

Figure 4: $M_{\rm sat}/M_{\rm host} = 0.1$: Angular momentum against time, normalized such that the $t = 0$ values are unity.

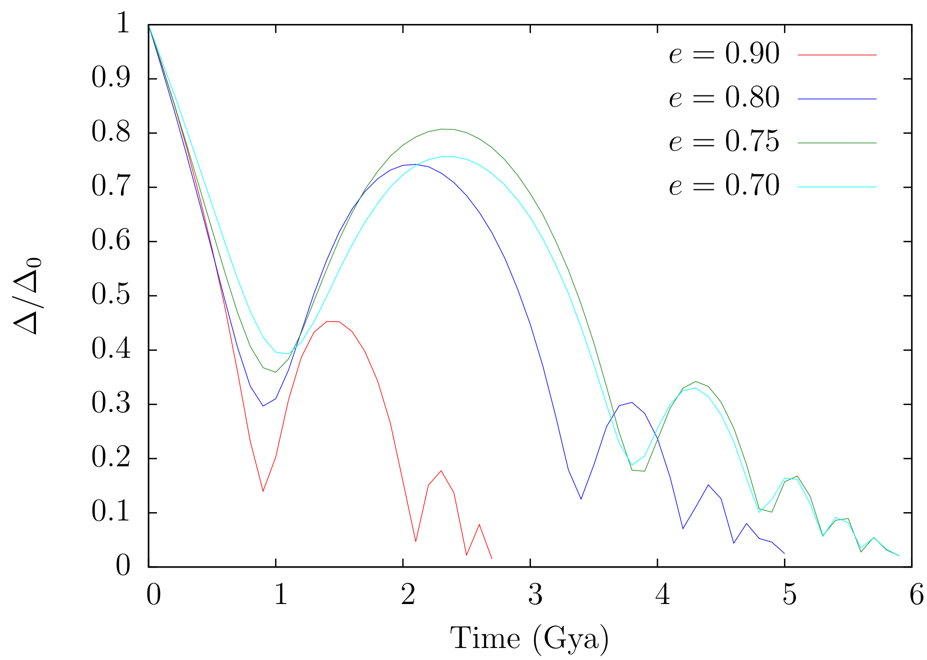

Figure 5: $M_{\rm sat}/M_{\rm host} = 0.1$: centre of mass separation between the galaxies Δ against time, normalized such that the $t = 0$ values are unity.

4.1.2 From other radii

For each of the runs the predicted merging time given by (3.1) was calculated and recorded at each snapshot. Table 4 shows the root mean squared (RMS) error of the prediction (reduced by 10% to account for baryons) against the recorded merging time. When calculating these values, two considerations were made. Firstly, the simulations with $e = 0.95$ were rejected because of the numerical issues. Secondly, the error was calculated only for ingoing trajectories (for reducing centre of mass separation). Equation (3.1) is not sensitive to the parity of the velocity/angular momentum of the satellite, so portions of the simulation where the galaxies are moving away from each other are not expected to generate sensible merging time predictions. Figures 6, 7 and 8 show the measured merging time for ingoing trajectories and the predictions for those snapshots.

We see large RMS errors for $M_{\rm sat}/M_{\rm host} < 0.3$ in Table 4. In general, the errors increase for a decrease in mass ratio. Figure 8 gives an instance of this, where the prediction is ≈ 4 Gya too large before the first pericentric passage. Notice that in all of the plots in this section, the prediction becomes more accurate (in terms of the absolute error) for smaller radii. While the predictions for $M_{\rm sat}/M_{\rm host} < 0.3$ are poor, and there are often large disagreements at multiple radii (see Figure 8), the predictions for $M_{\rm sat}/M_{\rm host} = 0.3$ are impressively robust. Furthermore, as displayed in Figures 6 and 7, the error is roughly constant throughout each run with $M_{\rm sat}/M_{\rm host} = 0.3$.

Run	RMS	Run	RMS	Run	RMS
30:95	—	10:95	—	10:70	21.6
30:85	0.7	10:90	4.5	10:65	4.6
30:60	1.7	10:85	4.6	05:95	—
30:40	1.5	10:80	9.4	05:85	25.9
30:0	1.7	10:75	10.7	05:75	19.2

Table 4: RMS (root mean squared error in Gya) between prediction and measurement over all radii, ingoing trajectories only. We reduced $\tau_{\rm merge}$ by 10% to account for the baryonic components.

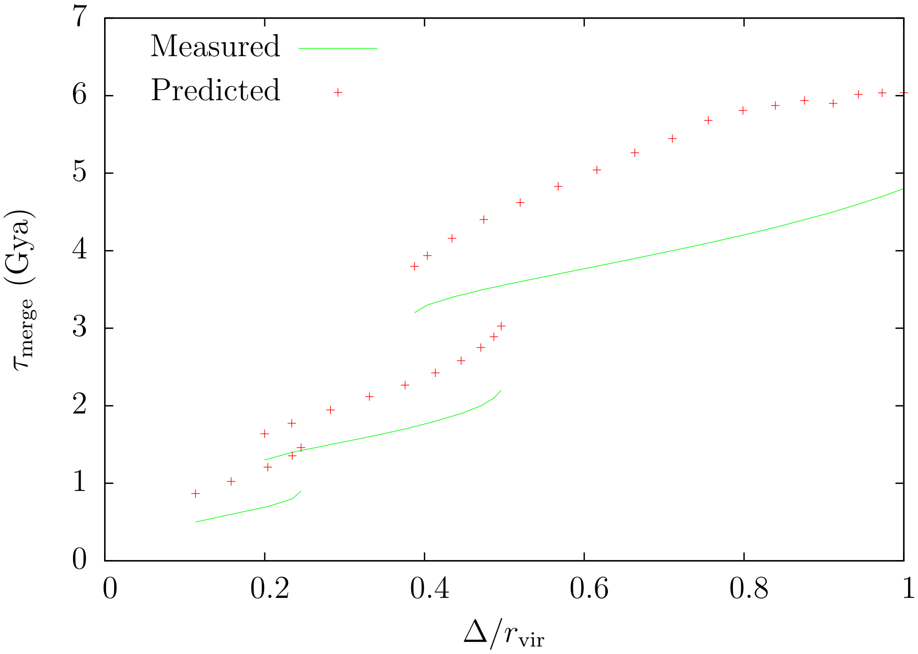

Figure 6: 30:60: Predicted and measured merging times against normalised centre of mass separation between the galaxies $\Delta/r_{\rm vir}$. We reduced $\tau_{\rm merge}$ by 10% to account for the baryonic components.

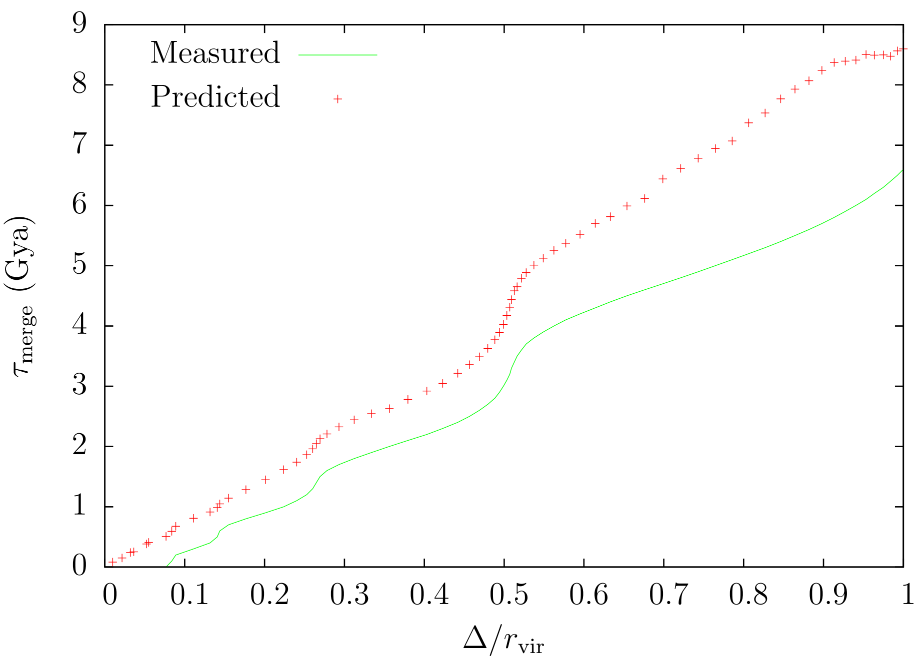

Figure 7: 30:40: Predicted and measured merging times against normalised centre of mass separation between the galaxies $\Delta/r_{\rm vir}$. We reduced $\tau_{\rm merge}$ by 10% to account for the baryonic components.

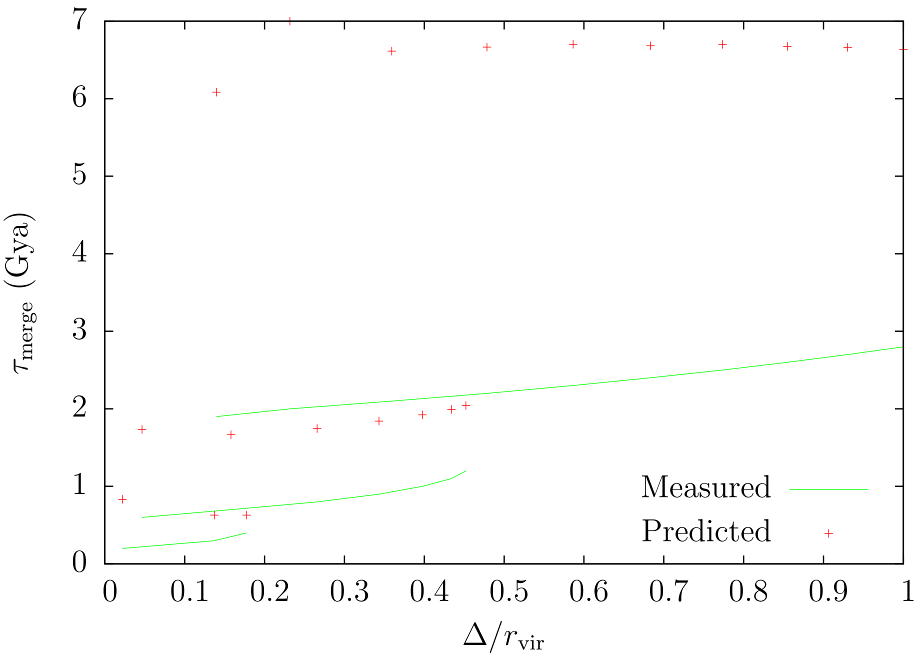

Figure 8: 10:90: Predicted and measured merging times against normalised centre of mass separation between the galaxies Δ/r_{vir}. We reduced τ_{merge} by 10% to account for the baryonic components.

4.2 Mass stripping

Figure 9 and Figure 10 show how the mass of the satellite changes over time in runs 30:95 and 05:75 respectively. In all cases, the halo of the satellite is initially stripped much faster than the bulge and more mass is stripped when the satellite is closer to the centre of the host that at other times. In the plots shown the mass of the satellite seems to increase immediately after a pericentric passage. This is a numerical artefact and not a physical phenomenon — the satellite is not believed to gain an appreciable amount of mass during an encounter.

There are two distinct regimes of stellar accretion during the merger. In the early stages of the merger baryonic matter is accreted to the host rather slowly. However, as the system evolves and the halo is stripped to $\approx 10\%$ of its initial value, the stellar bulge is accreted more quickly. In all of the runs the initial rate of stellar accretion is uniformly small and $\approx 10\%$ is lost during the early regime, but the rate of mass loss during the late regime depends on the mass of the satellite. For the $M_{\rm sat}/M_{\rm host} = 0.3$ satellites the loss of the stellar component in the late regime is almost immediate, but for less massive satellites it is more gradual.

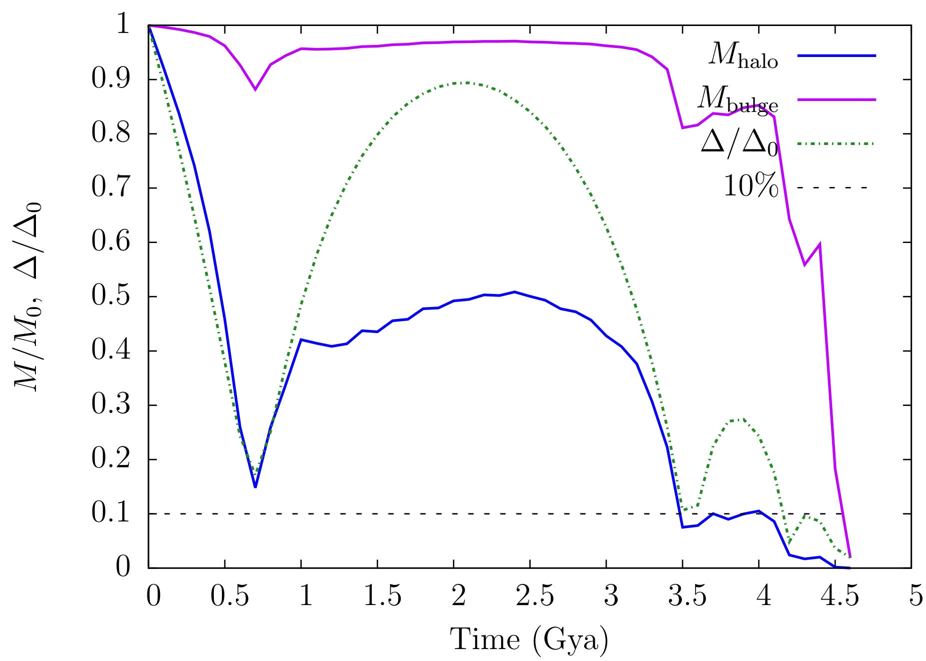

Figure 9: $M_{\rm sat}/M_{\rm host} = 0.3,\ e = 0.95$. Halo and bulge mass of the satellite against time with centre of mass separation between the galaxies Δ/Δ_0 over-plotted. All plots are normalised such that the $t = 0$ values are unity. Note the correlation between pericentric passages and mass stripping.

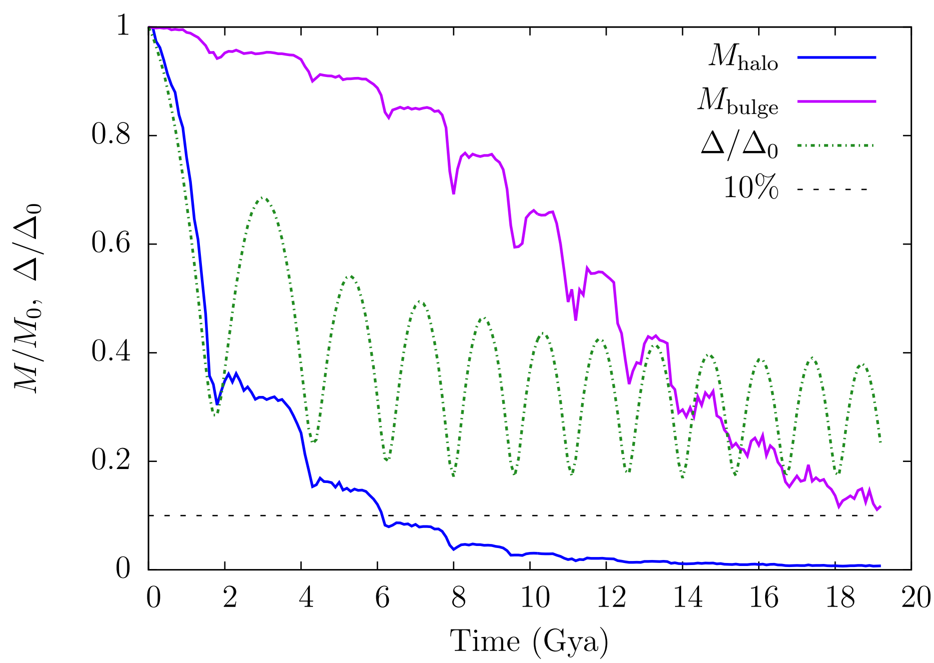

Figure 10: $M_{\text{sat}}/M_{\text{host}} = 0.05,\ e = 0.75$. Halo and bulge mass of the satellite against time with centre of mass separation between the galaxies Δ/Δ_0 over-plotted. All plots are normalised such that the $t = 0$ values are unity. Note the correlation between pericentric passages and mass stripping.

5 Discussion

The features outlined in 4 characterise the interplay between dynamical friction and tidal forces during the mergers. The dynamical friction force on a satellite is proportional to its mass, so it is more relevant in the $M_{\mathrm{sat}}/M_{\mathrm{host}} = 0.3$ systems than in the others. For eccentric trajectories the satellite will pass close to the centre of the host and tidal effects strip mass to produce the step-like losses in J. On the other hand, for more circular trajectories this is less so and the continual drag of dynamical friction reduces angular momentum more smoothly. Furthermore, dynamical friction causes the satellite's orbit to decay to the centre of the host, where tidal forces are most prominent. Simultaneously, tidal forces strip mass that in turn increases the dynamical friction force on the satellite [Fujii et al., 2006]. The discussions in this section will be centred on the relationship between these processes.

5.1 Merging times

5.1.1 Some considerations

Due to the issues with SUBFIND that occur when analysing the initial stages of the simulations, deductions from Table 3 are not particularly reliable. This can be seen by comparison with Table 4, where the prediction provided by (3.1) is more consistent with our simulations for the $M_{\mathrm{sat}}/M_{\mathrm{host}} = 0.1$ mergers than for the $M_{\mathrm{sat}}/M_{\mathrm{host}} = 0.05$ runs. On the other hand, the corresponding initial predictions for $M_{\mathrm{sat}}/M_{\mathrm{host}} = 0.1$ in Table 3 are often wildly imprecise and much further from our measurements than the $M_{\mathrm{sat}}/M_{\mathrm{host}} = 0.05$ runs. Again, this is because of the spurious measurements of the velocities of the satellites at the beginning of the simulations. To inhibit the effect of such anomalies we will focus our attention on the consistency of 3.1 when analysed at various radii.

It should be noted that one would expect systematically longer merging times from (3.1) than we have measured in this work. As mentioned in section 3.2.1, the definition of a merger in [Boylan-Kolchin et al., 2008] has a less direct dependence on the loss of mass of the satellite than the definition (3.4). Tidal stripping gives a more immediate contribution to the reduction of J than it does to $j = J/\mu$ that is used in [Boylan-Kolchin et al., 2008]. This is because for tidal stripping to cause a reduction in j, the velocities of stripped particles must be assimilated into the velocity profile of the host through encounters with host particles — this assimilation acts over a longer time scale to the stripping itself and is necessarily preceded it. Hence, in the presence of tidal stripping, we expect J to decay faster than j.

With the difference in definition it is difficult to speak conclusively about the accuracy of predictions based upon (3.1). The amount to which this difference in definition contributes to the disagreement in merging times is difficult to quantify without further measurement. In spite of this, we have gained some insight into the consistency of (3.1) when applied to starting radii $r < r_{\rm vir}$. The key aspect is that roughly constant error along ingoing trajectories in Figures 6, 7 and 8 indicate that (3.1) is indeed applicable to radii $r < r_{\rm vir}$. Further, the consistency remains intact for $r \ll r_{\rm vir}$, contrary to the suggestions in [Boylan-Kolchin et al., 2008]. Inferences from this must be made tentatively, because the exact mechanisms by which (3.1) differs from our measurements are yet to be established or quantified. It is argued below that tidal stripping is the main source of discrepancy, but we reiterate, until this is tested directly one must be careful about drawing conclusions.

5.1.2 The disagreement between prediction and simulation

We believe that the source of disagreement between the predictions based on (3.1) and our measurements is due to tidal stripping. The first point in support of this is the roughly constant disagreement between the predicted and measured merging times along ingoing trajectories. This indicates that the discrepancy between the prediction and our measurements is systematic. Further, as explained above, the definition used in this work will give systematically shorter merging times than (3.1) due to tidal stripping. This lends itself well to the idea that tidal stripping causes the discrepancy via the difference in definitions.

This notion is compounded by our data. Observe from Figures 6, 7 and 8 that the largest discrepancies appear along the initial ingoing trajectory. Relate this to Figures 9 and 10 and see that the radii at which the rate of mass loss is greatest are the same radii for which the discrepancy is greatest. Moreover, the simulations for which the prediction is closest to the measured merging time are those for which tidal stripping is least pertinent to the satellite's reduction in J relative to dynamical friction. That is, for $M_{\rm sat}/M_{\rm host} = 0.3$ and in particular for runs in which G030 is on trajectories of low eccentricity. It is for these systems that reductions in j, relative to reductions in μ, are most relevant to reductions in J. This is because, from the trajectories considered, these are the ones on which μ varies the slowest. Consequently it is for these systems that the definition of merger time based upon $J = \mu j$ (3.4) is closest to that of [Boylan-Kolchin et al., 2008].

5.2 Mass loss

In section 4.2 we see that there are two distinct regimes of stellar accretion during the merger. The bulge of the satellite remains $\lessapprox 10\%$ stripped until the halo is stripped by more than 90%, at which point the stellar accretion is quickened significantly. Figures 9 and 10 suggest that the rate at which the stellar component of the satellite is stripped in this second stage is related to the initial mass and trajectory of the satellite.

The dark matter halo of the satellite, being more diffuse than the stellar component, is less self-bound gravitationally per unit mass. This implies that the tidal radius of the halo is smaller than the bulge, when considered as a proportion of their respective virial radii, and so the halo loses mass to tidal effects more readily. In particular, note that the majority of the dark matter of the satellite is accreted by its first pericentric passage. Additionally, the bulge, being more self-bound than the halo, is more resistant to increases in its internal kinetic energy and the velocity dispersion of its constituents. These are the key reasons why the halo of the satellite is stripped prior to the bulge.

The gravitational potential due to the satellite is vastly dominated by the contribution of the dark matter component. This has a stabilizing effect on the stellar bulge, that resides at the minimum of the potential of the halo, making the bulge even more resistant to tidal forces. When the halo is stripped this is no longer the case and the stellar mass of the satellite is accreted. The rate of this accretion is related to the initial mass and trajectory of the satellite. Tidal forces are strongest near the centre of the host, within its scale length of 40 kpc $= 0.19\,r_{\rm vir}$, and so satellites that have remnants which orbit mostly outside this sphere lose stellar mass less rapidly than those that have orbits mostly interior to it. Note that, outside a sphere of radius $0.19\,r_{\rm vir}$ about the centre of the host, tidal forces on the satellite decrease in strength $\sim 1/r^3$ for increases in separation, so we proximity to this sphere is relevant to the rate of mass stripping.

The separation of the satellite remnant from the centre of the host in the late stages of the merger is determined by its specific orbital angular momentum. Hence the dependence on initial trajectory and mass. More massive satellites will lose orbital angular momentum more quickly and so, ceteris paribus, their corresponding remnants will retain less angular momentum and reside closer to the centre of the host. Further, the mass of the stellar component of the galaxies scales with total mass, so satellite's with larger initial mass will have remnants that are more massive and that lose orbital angular momentum faster due to dynamical friction. Lastly, the amount of orbital angular momentum retained by the remnant is related to the orbital angular momentum that it began with. Therefore eccentric orbits will have remnants that have more specific orbital angular momentum than for high circularity orbits. However, the effect of this on the rate of stripping is not entirely straightforward, because the trajectory of the satellite determines the pericentric distance of the orbit, which in turn is relevant to stripping.

6 Conclusions

In this work we ran 15 N-body simulations of dry, binary mergers between galaxies consisting of Hernquist profile dark matter halo and Hernquist profile stellar bulge. We used the N-body code GADGET [Springel, 2005] to run the simulations and the related package SUBFIND to identify the galaxies at each snapshot. We introduced our own definition of the merging time and, against the data gathered from our simulations, we tested the fitting formula for merging times (3.1) (reduced by 10% to account for the baryonic component) from [Boylan-Kolchin et al., 2008]. We compared (3.1) against our merging times measured from when the satellite crosses the virial radius of the host and for starting radii $r < r_{\mathrm{vir}}$. In addition we examined the rate of mass accretion to the host at different points in the merger.

Our results show that (3.1) consistently overestimates the merging times measured using the definition (3.4). These overestimations are greatest at the beginning of the merger, roughly constant along each ingoing trajectory of the satellite and generally decrease after each pericentric passage. The predictions of [Boylan-Kolchin et al., 2008] are most accurate for the systems with mass ratio $M_{\mathrm{sat}}/M_{\mathrm{host}} = 0.3$ and in general apply consistently well across all radii for this mass ratio. The predictions perform substantially less well for the systems with $M_{\mathrm{sat}}/M_{\mathrm{host}} < 0.3$ and worst for $M_{\mathrm{sat}}/M_{\mathrm{host}} = 0.05$ when averaged over all snapshots where the galaxies are moving together. From our examination of the loss of mass of the satellite we see that the majority of the dark matter of the satellite is accreted to the host after the first pericentric passage. Further, we find that an appreciable amount of stellar mass ($> 10\%$) is not stripped from the satellite until after the halo of the satellite is almost completely ($\approx 90\%$) removed. When the stellar mass is eventually accreted, it is at a rate dependent on the initial mass and trajectory of the satellite. From this emerge two distinct regimes of stellar accretion from the satellite to the host: the first gradual, while the halo remains above 90% of its initial mass, the second more rapid and sometimes almost immediate.

We deduce that tidal stripping is the main cause for the overestimation made by (3.1) when considered against our measurements. Essentially, we argue that the predictions of (3.1) are inappropriate for our definition of merging time (3.4). This is because our definition is more sensitive to tidal stripping of mass from the satellite than the definition in [Boylan-Kolchin et al., 2008]. Additionally, we find that the variation in rate of stellar mass accretion between the systems considered is due to variations in the initial mass trajectory of the satellite.

Our conclusions regarding (3.1) are limited by two considerations. Firstly, our analysis was jaded by the erratic behaviour of SUBFIND, which gave unexpected values for the velocity of the satellite in the initial stages of the simulations. This is somewhat mitigated by the roughly constant discrepancy between prediction and results across radii, indicating that SUBFIND only has issues with the initial portion of the simulations. Nevertheless, this is a potential source of error in our results. Secondly, the difference in definition between this work and [Boylan-Kolchin et al., 2008] could be very significant. In the time available we were not able to quantify this difference, so we cannot make serious quantitative judgements of the accuracy of (3.1). We do, however, come to some qualitative conclusions about the consistency of (3.1) when applied to radii $r < r_{\mathrm{vir}}$. In particular, we conclude that merging time predictions by (3.1) are robust for $r < r_{\mathrm{vir}}$. We hope that the findings of this work will useful for semi-analytic models of structure formation and for observations of merging pairs.

7 Suggestions for further work

In order to assess the accuracy of (3.1) rigorously, the discrepancy between the definition (3.4) and the one in [Boylan-Kolchin et al., 2008] needs to be quantified. An approach to this problem could involve isolating the variation of either μ or j over a merger and relating these to the variation in $J = \mu j$. Doing this would yield quantitative insight into the systematic difference between the definitions. In turn, one would be able to use the data presented here to check the accuracy of (3.1) more thoroughly. With the output from our simulations and the data presented here, this is an attainable goal. However, we were not able to perform the requisite analysis in time for submission. A second, more intensive approach is to fit a formula similar to (**??**) or (2.5) to our data and then compare this with (3.1). This approach is comprehensive and would generate predictions with respect to the definition (3.4), but it is less direct than the first approach and would not tell us *why* the observed discrepancies have arisen.

An additional direction in which this work could be extended is to further explore the indicators of tidal stripping. If a satellite is larger than its tidal radius then it will experience mass loss in the presence of gravitational tidal forces. The tidal radius of a body is related to the contours of zero force throughout the system. We believe that it would be interesting to investigate whether the area bounded by the contours of zero force that enclose the satellite at a given time is related to the rate of stripping. For instance, we would expect a reduction in the area bounded by these contours to be related to reduction in mass of the satellite.

Acknowledgements

I would like to thank Ben and Debora for their help and guidance with this project and, most of all, for their patience with me. It hasn't been easy, but it has been a fantastic learning experience and I've thoroughly enjoyed it.

This work was performed using the Darwin Supercomputer of the University of Cambridge High Performance Computing Service (http://www.hpc.cam.ac.uk/), provided by Dell Inc. using Strategic Research Infrastructure Funding from the Higher Education Funding Council for England and funding from the Science and Technology Facilities Council.

References

[Barnes and Hernquist, 1992] Barnes, J. E. and Hernquist, L. (1992). Dynamics of interacting galaxies. *Annu. Rev. Astron. Astrophys.*, 30:705–742.

[Benson, 2005] Benson, A. J. (2005). Orbital parameters of infalling dark matter substructures. *MNRAS*, 358:551–562.

[Bertone and Conselice, 2009] Bertone, S. and Conselice, C. J. (2009). A comparison of galaxy merger history observations and predictions from semi-analytic models. *MNRAS*, 396:2345–2358.

[Binney and Tremaine, 1987] Binney, J. and Tremaine, S. (1987). *Galactic Astronomy and Dynamics*, chapter 7, pages 417–483. Princeton University Press, Princeton, NJ.

[Boylan-Kolchin et al., 2008] Boylan-Kolchin, M., Ma, C.-P., and Quataert, E. (2008). Dynamical friction and galaxy merging time-scales. *MNRAS*, 383:93–101.

[Chandrasekhar, 1943] Chandrasekhar, S. (1943). Dynamical Friction. I. General Considerations: the Coefficient of Dynamical Friction. *ApJ*, 97:255.

[Davis et al., 1985] Davis, M., Efstathiou, G., Frenk, C. S., and White, S. D. M. (1985). The evolution of large-scale structure in a universe dominated by cold dark matter. *ApJ*, 292:371–394.

[Dehnen, 2001] Dehnen, W. (2001). Towards optimal softening in three-dimensional N-body codes - I. Minimizing the force error. *MNRAS*, 324:273–291.

[Efstathiou and Silk, 1983] Efstathiou, G. and Silk, J. (1983). The formation of galaxies. *Fundamentals of Cosmic Physics*, 9:1–138.

[Fujii et al., 2006] Fujii, M., Funato, Y., and Makino, J. (2006). Dynamical Friction on Satellite Galaxies. *Publ. Astron. Soc. Japan*, 58:743–752.

[Hernquist, 1990] Hernquist, L. (1990). An analytical model for spherical galaxies and bulges. *ApJ*, 356: 359–364.

[Jiang et al., 2008] Jiang, C. Y., Jing, Y. P., Faltenbacher, A., Lin, W. P., and Li, C. (2008). A Fitting Formula for the Merger Timescale of Galaxies in Hierarchical Clustering. *ApJ*, 675:1095–1105.

[Mihos, 2000] Mihos, C. (2000). Galaxies: Interactions and Mergers. *Encyclopedia of Astronomy and Astrophysics*, page 2623.

[Mo and White, 2010a] Mo, H.; van den Bosch, F. and White, S. (2010a). *Galaxy Formation and Evolution*, chapter 1, pages 1–24. Cambridge University Press, Cambridge, UK.

[Mo and White, 2010b] Mo, H.; van den Bosch, F. and White, S. (2010b). *Galaxy Formation and Evolution*, chapter 544-573, pages 1–24. Cambridge University Press, Cambridge, UK.

[Navarro et al., 1995] Navarro, J. F., Frenk, C. S., and White, S. D. M. (1995). The assembly of galaxies in a hierarchically clustering universe. *MNRAS*, 275:56–66.

[Springel, 2005] Springel, V. (2005). The cosmological simulation code GADGET-2. *MNRAS*, 364:1105–1134.

[Springel et al., 2005] Springel, V., Di Matteo, T., and Hernquist, L. (2005). Modelling feedback from stars and black holes in galaxy mergers. *MNRAS*, 361:776–794.

[Springel et al., 2001] Springel, V., White, S. D. M., Tormen, G., and Kauffmann, G. (2001). Populating a cluster of galaxies - I. Results at $z = 0$. *MNRAS*, 328:726–750.

[Toomre, 1977] Toomre, A. (1977). *The Evolution of Galaxies and Stellar Populations*, page 401. New Haven: Yale Univ. Observatory.

[Toomre and Toomre, 1972] Toomre, A. and Toomre, J. (1972). Galactic Bridges and Tails. *ApJ*, 178:623–666.

[White, 1976] White, S. D. M. (1976). A note on the minimum impact parameter for dynamical friction involving spherical clusters. *MNRAS*, 174:467–470.

[White and Rees, 1978] White, S. D. M. and Rees, M. J. (1978). Core condensation in heavy halos - A two-stage theory for galaxy formation and clustering. *MNRAS*, 183:341–358.

[Zentner et al., 2005] Zentner, A. R., Berlind, A. A., Bullock, J. S., Kravtsov, A. V., and Wechsler, R. H. (2005). The Physics of Galaxy Clustering. I. A Model for Subhalo Populations. *ApJ*, 624:505–525.

Appendix

Measuring merging times

Below is a short code that I wrote in C to calculate the merging time and error. It is part of a larger piece that loops over all SUBFIND output and calculates various properties of the galaxies for each snapshot. The integer `i` is the snapshot number, `J` is the relative angular momentum of the satellite about the centre of mass of the host and `JInitial` is its $t = 0$ value.

```c
double J, JInitial, Tmerge, error;
int q, p, z, numsnapsup, numsnapsdown;

q = 0;
p = 0;
z = 0;
numsnapsdown = 0;
numsnapsup = 0;
Tmerge = 0.0;
error = 0.0;

if (J < JInitial*0.01)
{
  if (z>0) numsnapsup = q;
  z++;
  if (p == 0)
  {
    Tmerge = i*0.1;
    error = 0.1*(numsnapsup + numsnapsdown);
  }
    p++;
    q = 0;
} else {
      if (!(p==0)) numsnapsdown = p;
      p = 0;
      Tmerge = 0.0;
      /* to indicate that the merger hasn't yet happened */
      q++;
}
```